

Feature article

Improper, blue-shifting hydrogen bond

Pavel Hobza¹, Zdenek Havlas²

¹J. Heyrovský Institute of Physical Chemistry, Academy of Sciences of the Czech Republic, 182 23 Prague 8, Czech Republic

^{1,2}Center for Complex Molecular Systems and Biomolecules, 182 23 Prague 8, Czech Republic

²Institute of Organic Chemistry and Biochemistry, Academy of Sciences of the Czech Republic, 166 10 Prague 6, Czech Republic

Received: 25 February 2002 / Accepted: 2 June 2002 / Published online: 16 September 2002

© Springer-Verlag 2002

Abstract. The spectral manifestation and the nature of improper, blue-shifting hydrogen-bonded complexes are entirely different from those of standard hydrogen-bonded complexes. While the latter class of complexes is characterized by an elongation of the $X-H$ bond and a concomitant red shift of the respective stretch frequency, a contraction of the $X-H$ bond and a blue shift of the $X-H$ stretch frequency are typical for the former class of complexes. Both classes of complexes exhibit electron-density transfer from the proton acceptor to the proton donor. In the case of hydrogen-bonded complexes, the electron-density transfer is mostly larger than in the improper complexes. The role of the charge transfer and electrostatic interaction is discussed. The importance of the charge transfer is documented by natural bond orbital analysis, orbital interaction diagrams, and by the insufficient description of the interaction by the electrostatic model only.

Key words: Hydrogen bond – Improper, blue-shifting hydrogen bond – Properties – Nature – Vibrational spectroscopy

1 Introduction

One of the strongest and the most common types of noncovalent bond is the hydrogen bond. It is difficult to define a hydrogen bond in a way that would cover all the features ascribed to it by the different branches of science. The most common definition describes it as an attractive interaction between two species (atoms, groups, or molecules) in a structural arrangement where the hydrogen atom, covalently bound to a more electronegative atom of one species, is noncovalently bound to a place with an excess of electrons of the other

species. This definition does not specify the nature of the hydrogen bond, which makes the definition quite general, but not in concrete terms.

The hydrogen bond plays a key role in chemistry, physics, and biology and its consequences are enormous. Hydrogen bonds are responsible for the structure and properties of water, an essential compound for life, as a solvent and in its various phases. Further, hydrogen bonds also play a key role in determining the shapes, properties, and functions of biomolecules. For a survey the reader is referred to recently published monographs on hydrogen bonding [1, 2, 3]. The term “hydrogen bond” was probably used first by Pauling in his article on the nature of the chemical bond [4].

The hydrogen bond is a noncovalent bond between the electron-deficient hydrogen and a region of high electron density. Most frequently, a hydrogen bond is of the $X-H...Y$ type, where X is the electronegative element and Y is the place with the excess of electrons (e.g., lone electron pairs, π electrons). Hydrogen bonds having $X, Y = F, O,$ and N are the most frequent and best studied [1, 2, 3]. Recently, the $X-H...n\pi$ hydrogen bonds (for $X = O$ and C) were also detected [5, 6, 7, 8, 9, 10, 11, 12].

Despite of the enormous amount of literature a question arises again and again: Does the hydrogen bond represent some special type of noncovalent interaction? Looking from the quantum theoretical horizon the answer is unambiguous – no. Any type of hydrogen bonding is stabilized by the same energy components like any other noncovalent bonding. The most important electrostatic contribution is accompanied by induction and dispersion ones. These attractive terms are balanced by an exchange–repulsion. There is nothing special on this energy composition of the total interaction and from the point of view of intermolecular noncovalent bonding the hydrogen bond does not form any special class. Evidently, the only peculiarity of the hydrogen bond comes from the structural form, directionality, and its importance in chemistry and biology. It is the shared hydrogen atom between two electronegative atoms (in the most common complexes) which causes the typical,

Correspondence to: P. Hobza
e-mail: hobza@indy.jh-inst.cas.cz

almost linear $X-H...Y$ arrangement. Further, sharing of very light hydrogen between two electronegative atoms results in a rather dramatic change in the properties of the $X-H$ covalent bond. The perturbation caused by the complex formation is astonishingly pronounced when one considers the relative weakness of the hydrogen bond. This bond becomes weaker upon formation of the hydrogen bond and this weakening is the key factor for understanding the changed properties of the $X-H$ stretch vibrational frequency. A shift to lower frequencies (called red shift) represents the most important, easily detectable (in liquid, gas, and solid phases) manifestation of the formation of a hydrogen bond. Note that these “significant” changes of molecular properties upon complex formation are actually quite small: the change in energy, geometry, IR frequencies, and electron density is 2 or more orders of magnitude smaller than typical changes in chemical processes. The red shift of the $X-H$ stretch vibration, which varies between several tens and hundreds of wavenumbers, represented until recently unambiguous information on the formation of hydrogen bonds.

It must be stressed that IR spectroscopy is the most essential experimental technique for investigating the hydrogen-bonding phenomenon and other techniques (e.g., NMR, UV and X-ray) are less important and less potent in yielding an experimental evidence for hydrogen-bond formation.

We can summarize that the characteristic features [3] of $X-H...Y$ hydrogen bond are

1. The $X-H$ covalent bond stretches and correlates with the strength of the hydrogen bond.
2. A small amount of electron density (0.01–0.03e) is transferred from the proton-acceptor (Y) to the proton-donor molecule ($X-H$).
3. The band which corresponds to the $X-H$ stretch shifts to lower frequency (red shift), increases in intensity, and broadens. The value of the red shift and the strength of the hydrogen bond correlate as well.

A frequently asked question concerns the small amount of electron density transferred during the hydrogen-bonded complex formation (see earlier). It must be kept in mind that chemical processes are connected with small changes of the total electron density. Larger changes are observed only locally and are caused by a few electrons. For weak molecular interaction the changes are very small.

In the last few years several pieces of evidence were collected [13] which indicated that the $X-H...Y$ arrangement can be accompanied by opposite geometrical and spectral manifestation. Instead of elongation of the $X-H$ bond accompanied by a red shift of the $X-H$ stretch vibration, the contraction of this bond and the blue shift of the respective stretch vibration were detected. Moreover, the intensity of the $X-H$ stretch vibration often decreased upon formation of the $X-H...Y$ contact, again in contrast to standard hydrogen bonding. The common feature of this novel type of bonding, called improper, blue-shifting hydrogen bonding, and standard hydrogen bonding is the charge transfer from the proton acceptor to the proton donor.

The goal of this review is to clarify various aspects of intermolecular bonding of proton donors and proton acceptors and to explain the nature of the standard (red-shifting) hydrogen bonding as well as the improper, blue-shifting hydrogen bonding. We refer in this overview not only to results and conclusions published in the cited references but also to some new, original views published for the first time.

2 History and survey of improper, blue-shifting hydrogen bonding

The first experimental evidence of a blue shift of the $X-H$ stretch frequency upon formation of a complex was obtained in 1980 by Trudeau et al. [14], who measured association of fluoroparaffins containing the $-CHF_2$ groups with various proton acceptors and found a shift of the CH stretch frequency to higher values. This unusual behavior was explained by the location of the hydrogen and fluorine atoms at the same carbon resulting in a decrease in the acidity of the hydrogen atom. Further experimental evidence appeared in 1989 when Budešinský et al. [15] reported the blue shift of chloroform upon complexation with trimethylmethane. The third observation of the blue shift was reported in 1997 by Boldeskul et al. [16], who measured the IR spectra of chloroform, deuteriochloroform, and bromoform in mixed systems containing proton acceptors such as carboxy, nitro and sulfo groups. The first systematic investigation of the blue shift of the $X-H$ stretch frequency in $X-H...Y$ complexes was a theoretical study of the interaction of benzene with C-H proton donors [17]. It was shown that the formation of benzene...H-X ($X = -CH_3, -CCl_3, -C_6H_5$) complexes leads to a C-H bond contraction and an increase in the respective stretch frequency (blue shift). Because the most important features (the shortening of the proton donor C-H bond and the blue shift) were opposite to those characteristic of classical hydrogen bonds (the elongation of the proton donor $X-H$ bond and the red shift), we originally called this specific bonding type an “anti-hydrogen bond”; because of the confusing meaning of this term we substituted it later [13] by the present term “improper, blue-shifting” hydrogen bond.

The blue shift of the C-H stretch frequency was first detected in solution [14, 15, 16]. Direct evidence of the blue shift in the gas phase was missing until 1999, when a complex between fluorobenzene and chloroform was investigated using double-resonance IR ion-depletion spectroscopy [18]. The experimental value of the blue shift of the chloroform C-H stretch frequency (14 cm^{-1}) agreed well with the theoretical prediction (12 cm^{-1}), using a good quality ab initio treatment. The same technique was later used for a complex of fluorobenzene with fluoroform and again the agreement between the experimental blue shift and its theoretical prediction was good [19]. The blue shift of the C-H stretch frequency was also theoretically predicted for C-H...O contacts. The first system investigated was fluoroform...oxirane [20], where a significant blue shift of 30 cm^{-1} was predicted. The family of C-H...O complexes exhibiting a

blue shift of the C–H stretch frequency upon complexation was later extended [21] to dimers of $F_nH_{3-n}CH$ with H_2O , CH_3OH , and H_2CO . These theoretical calculations predicted the largest blue shift of 47 cm^{-1} for the $F_3CH\dots OHCH_3$ complex. A very large blue shift of the C–H stretch frequency, more than 100 cm^{-1} , was detected recently from IR spectra of $X^- \dots H_3CY$ ionic complexes ($X = Cl$, $Y = Br$; $X, Y = I$), which were also thoroughly investigated theoretically [22], in excellent agreement with the experimental values.

Up to now various types of improper, blue-shifting hydrogen bonds containing the $X-H$ proton donor have been detected experimentally in the gas or liquid phases and/or found theoretically: $C-H\dots\pi$ [17, 18, 19], $C-H\dots O$ [15, 16, 20, 21, 22, 23, 24, 25, 26, 27, 28, 29], $C-H\dots F$ [30], $C-H\dots X^-$, $Si-H\dots N$ [31].

3 Nature of standard and improper, blue-shifting hydrogen bonding

3.1 Electrostatic and charge-transfer models

What is the driving force for the formation of a hydrogen bond? There are two models describing the mechanism of hydrogen bonding: electrostatic and charge transfer. The first model explains the formation of a hydrogen bond using energy arguments: elongation of the $X-H$ bond increases the dipole of a subsystem and thus also the dipole–dipole attraction between proton donor and proton acceptor. Consequently, the total stabilization energy becomes larger. This model explains geometrical, energetical, and also vibrational characteristics of the standard hydrogen-bonded complex. Renaissance of the model was brought recently by Masunov et al. [24], who investigated the changes in the proton donor in the electrostatic field of the proton acceptor. Is it therefore necessary to include the concept of charge transfer? Let us remind ourselves that the phenomenon of charge transfer is rather vague. We cannot detect it directly and its theoretical justification is not unambiguous. The first clear evidence supporting the charge-transfer concept came from Coulson [32], who showed that without allowing electron transfer from the proton acceptor to the proton donor one cannot explain the dramatic increase in intensity of the $X-H$ stretch vibration upon formation of a hydrogen bond. Later the concept of charge transfer was proven by using the natural bond orbital (NBO) analysis. Reed et al. [33] performed the NBO analysis for several typical hydrogen-bonded systems and demonstrated charge transfer from the lone pairs of the proton acceptors to the $X-H$ σ^* antibonding orbitals of the proton donor. An increase in the electron density in the antibonding orbitals weakens the $X-H$ covalent bond, which leads to its elongation, accompanied by the concomitant lowering of the $X-H$ stretch frequency. The NBO analysis thus represents a very useful technique for studying the mechanism of hydrogen bonding. It must be mentioned that atoms-in-molecules analysis [34] gives very similar results and can also be used for these purposes [35, 36].

How do the two models describe the formation of the improper, blue-shifting hydrogen bond? Similarly as in the case of the classical hydrogen bonding. Both models provide useful information about the formation of the improper, blue-shifting hydrogen bond. The electrostatic model describes the increased dipole–dipole attraction in some complexes, in which a contraction of the $X-H$ bond leads to an increase in the $X-H$ proton-donor dipole moment. This is not speculation – in the case of CHF_3 the contraction of the C–H bond increases the dipole moment of the subsystem [20]. The applicability of both models is demonstrated in the following paragraphs for various classes of molecular complexes having (within the class) the same proton acceptor.

The NBO analysis required for the discussion of the charge-transfer model was fully described in the original works cited. The electric field calculations were, however, made for the purpose of this overview and their technical details are as follows. The electrostatic field was modeled by point charges calculated by the Merz–Kollman fitting procedure (included in the Gaussian 98 code) at the MP2/SDD** level. Two sets of charges were used for comparison of the sensitivity of the resulting structures to the values of the charges. First, the charges were evaluated in the dimer, and, second, the charges were calculated for the proton-acceptor molecule in the geometry of the dimer. The charges were located at the position of the atoms of the proton-acceptor molecule and the distances of these positions to the hydrogen atom(s) of the proton-donor molecule were fixed in the optimization procedure. Also the orientation of the proton-donor molecule to the positions of the proton-acceptor molecule was fixed, otherwise the optimization would lead to the artificial collapse of the charges with the proton-donor molecule owing to the electrostatic forces. The optimization of all the proton donor internal coordinates was successfully performed to tight accuracy using the Gaussian 98 GAUOPT program. Let us note finally that the model of the electrostatic field and the method of the optimization of the molecules in this field is neither unique nor exact. We have tested many possibilities and the model presented here gives the best coincidence between changes in the real complexes and in the electrostatic field.

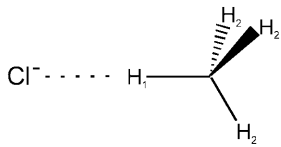
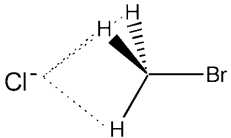
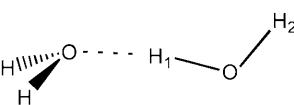
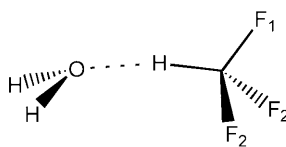
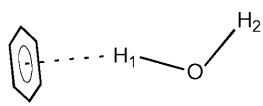
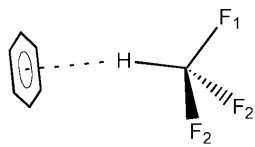
The results of the optimization of the proton-donor structures exposed to the electrostatic field of point charges of the proton acceptor are given in Table 1.

3.2 $Cl^- \dots HCH_3$ and $Cl^- \dots H_3CBr$ complexes

The structures of both complexes are shown in Fig. 1. $Cl^- \dots HCH_3$ is a standard hydrogen-bonded complex. The NBO analysis revealed the electron-density transfer (EDT) from the lone electron pairs of the halogen ion to the C–H σ^* antibonding orbital of the C–H bond, which is directed to the Cl^- ion. The C–H bond becomes weaker, is elongated, and its stretch frequency is lowered.

The $Cl^- \dots H_3CBr$ complex is entirely different. The dominant EDT (again from the lone electron pairs of the

Table 1. Geometrical parameters of proton-donor molecules (distances in angstroms, angles in degrees) in the monomer and their changes influenced by dimer formation and by the electrostatic field of the proton acceptor modeled by point charges calculated according to the Merz–Kollman procedure (in the dimer, q_{MK}^{dimer} , and for the monomer in the dimer geometry, $q_{MK}^{monomer}$)

| system | geom. parameter p | p (monomer) | Δp (dimer) | Δp (q_{MK}^{dimer}) | Δp ($q_{MK}^{monomer}$) |
|---|---------------------|---------------|--------------------|---------------------------------|-----------------------------------|
|  | $r(C-H_1)$ | 1.0888 | 0.0062 | 0.0009 | 0.0011 |
| | $r(C-H_2)$ | 1.0888 | 0.0029 | 0.0022 | 0.0021 |
| | $\alpha(H_1-C-H_2)$ | 109.47 | 0.67 | 0.37 | 0.39 |
|  | $r(C-H)$ | 1.0860 | -0.0056 | -0.0035 | -0.0038 |
| | $r(C-Br)$ | 1.9559 | 0.0617 | 0.0336 | 0.0388 |
| | $\alpha(H-C-Br)$ | 107.62 | -1.05 | -0.76 | -0.94 |
|  | $r(O-H_1)$ | 0.9634 | 0.0062 | 0.0016 | 0.0017 |
| | $r(O-H_2)$ | 0.9634 | -0.0007 | -0.0007 | -0.0007 |
| | $\alpha(H_1-O-H_2)$ | 104.60 | 0.30 | -0.30 | -0.32 |
|  | $r(C-H)$ | 1.0873 | -0.0020 | -0.0031 | -0.0028 |
| | $r(C-F_1)$ | 1.3474 | 0.0036 | 0.0025 | 0.0022 |
| | $r(C-F_2)$ | 1.3474 | 0.0047 | 0.0043 | 0.0039 |
| | $\alpha(H-C-F_1)$ | 110.54 | 0.91 | 0.73 | 0.68 |
| | $\alpha(H-C-F_2)$ | 110.54 | 0.27 | 0.30 | 0.26 |
|  | $r(O-H_1)$ | 0.9634 | 0.0024 | 0.0008 | 0.0011 |
| | $r(O-H_2)$ | 0.9634 | 0.0003 | -0.0003 | -0.0003 |
| | $\alpha(H_1-O-H_2)$ | 104.60 | -0.94 | -0.78 | -0.88 |
|  | $r(C-H)$ | 1.0875 | -0.0041 | -0.0025 | -0.0026 |
| | $r(C-F_1)$ | 1.3473 | 0.0034 | 0.0024 | 0.0027 |
| | $r(C-F_2)$ | 1.3473 | 0.0031 | 0.0022 | 0.0023 |
| | $\alpha(H-C-F_1)$ | 110.54 | 0.37 | 0.25 | 0.28 |
| | $\alpha(H-C-F_2)$ | 110.54 | 0.33 | 0.25 | 0.28 |

Cl^- ion) is now directed into the $C-Br$ σ^* antibonding orbital, which results in the $C-Br$ bond elongation. This elongation leads to a geometrical reorganization of the CH_3Br molecule. The $C-H$ bonds are contracted and the $C-H$ stretch frequencies are blue-shifted. The $Cl^- \dots H_3CBr$ complex exhibits both the largest $C-X$ bond elongation and the greatest $C-H$ vibrational frequency blue shift among all the complexes studied up to now. An important difference between both complexes concerns the dominant geometry change. In the former complex, it occurred at the CH bond closest to the proton acceptor, while in the latter complex, the dominant geometry change is localized at the remote (nonparticipating) part of the proton donor.

The electrostatic field of the chlorine anion properly polarizes both partners (Table 1) and in both cases the

correct behavior of the proton acceptor results. This means the field induces elongation in the former case and contraction in the latter case. The elongation in the case of the standard hydrogen-bonded complex is, however, strongly underestimated and also contraction in the improper hydrogen-bonded complex is roughly half the value of the complex. Also the geometrical changes in the remote part of the proton donor are not completely reproduced by the electrostatic field alone and larger disagreement is seen in the improper hydrogen-bonded complex. The elongation of the $C-Br$ bond in the complex is twice as large as that predicted by the effect of the electric field. Evidently the charge transfer to the σ^* $C-Br$ antibonding orbital is undisputable.

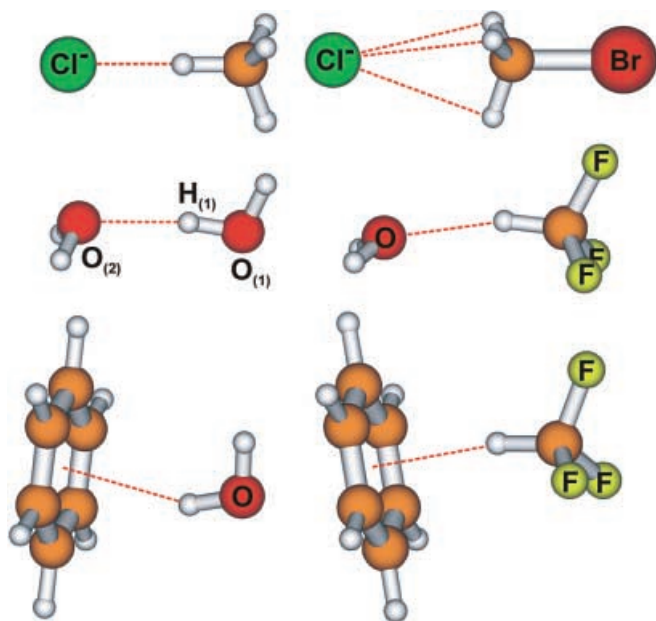


Fig. 1. Structures of complexes investigated

3.3 $H_2O...HOH$ and $H_2O...HCF_3$ complexes

The structures of both complexes are presented in Fig. 1. Let us first discuss the results of the NBO analysis for the hydrogen-bonded water dimer. The dominant part of the EDT is shifted from the oxygen $O_{(2)}$ lone pairs mainly to the $O_{(1)}-H_{(1)}$ antibonding σ^* orbital. The extra electron density weakens this O–H bond, resulting in its elongation and a concomitant red shift of its O–H stretch frequency. The situation with the $H_2O...HCF_3$ complex is, however, different. There is practically no EDT into the C–H antibonding σ^* orbital of fluoromethane. The EDT is directed to the lone pairs of the fluorine atoms. In addition to the intermolecular EDT, the electron density of fluoromethane undergoes an internal rearrangement. How should we interpret the NBO results for the $H_2O...HCF_3$ complex? The dominant feature of the overall EDT is the increase in the electron density at lone electron pairs of all the fluorine atoms in fluoromethane. This is the primary effect which causes elongation of all the C–F bonds. The elongation induces structural reorganization of the CHF_3 subsystem including contraction of the C–H bond. We conclude that the hydrogen bonding in the $H_2O...HCF_3$ complex is markedly different from the water dimer: the hydrogen bond in the latter complex is standard, while the hydrogen bond in the former is improper, blue-shifting. For these complexes it is again possible to localize the different position of the dominant geometry change: O–H bond in the case of the hydrogen-bonded water dimer and C–F bonds in the case of the improper hydrogen-bonded $H_2O...HCF_3$ complex.

The effect of the electric field of the proton acceptor is very similar to that found for the previous complexes. The field induces the geometry changes of the proton donor in the correct direction, but the changes are strongly underestimated in the case of the

hydrogen-bonded water dimer and the shortening of the C–H bond in the improper hydrogen-bonded complex is too great.

3.4 $Benzene...HOH$ and $benzene...HCF_3$ complexes

The structures of both complexes are depicted in Fig. 1. The former complex is again a standard hydrogen-bonded one, while the latter exhibits improper hydrogen bonding. The NBO analysis reveals a clear difference between them. The dominant part of the EDT from the benzene π molecular orbitals (MOs) in the former complex is directed to the OH σ^* antibonding orbital directed to the π system of benzene and only a small portion (about one-tenth) is directed to the other OH bond. An increase in the electron density in the OH antibonding orbital results in its elongation and a rather large red shift of the O–H stretch frequency. The situation in the latter complex is completely different and there is practically no EDT to the CH region of proton donor; its dominant part goes to the lone electron pairs of all the fluorine atoms. This electron density increase is followed by the structural reorganization of the fluoromethane subsystem, specifically elongation of all the C–F bonds and contraction of the C–H bond (similar to the $H_2O...HCF_3$ complex). By considering the (isolated) deformed subsystem and performing the vibrational analysis we found a rather large blue shift of the C–H stretch frequency (with respect to the C–H stretch frequency in the optimized isolated subsystem). The shift is almost equal to the shift detected in the complex, which supports the assumption that the shift in the complex is mainly due to the structural reorganization of fluoromethane. The NBO analysis also successfully describes bonding in the improper blue-shifted benzene... $HCCl_3$ complex.

If the water or fluoromethane is placed in the electrostatic field of the benzene subsystem, the predicted geometrical changes are again in the same direction as in the complexes (except very small changes of the remote O–H bond distance and H–O–H angle in the case of the benzene–water complex). Again, the change in the O–H bond distance, involved in the hydrogen bond of the classical benzene–water complex, is strongly underestimated compared to the change in the real complex. In the case of the improper benzene... HCF_3 complex, the electric field underestimates the shortening of the H–C bond by about half; the C–F bond elongation is also underestimated.

Note that the results of the optimization of the proton donors exposed to the electrostatic field of the proton acceptor are not very sensitive to the small variation of the charges. The point charges evaluated for the dimer or for the proton acceptor monomer provide essentially the same changes in the proton donor structure (Table 1).

From the analysis of the electrostatic and charge-transfer models in the complexes (as well as in other complexes with hydrogen bonding and improper hydrogen bonding not mentioned in this overview), we can conclude that the electrostatic field itself cannot describe

the changes in the proton-donor molecules and an additional mechanism, electron transfer, must be supplemented for the total reorganization of the proton-donor molecules in the complexes. We are aware of the fact that the model for the electrostatic field is imperfect and the polarization and exchange effects are neglected. These effects are, however, less important. The electrostatic field fails sometimes completely to interpret the geometry changes in the proton donor. This was documented in our recent article [27], where the bonding between HCX_3 and water was studied. For $X = \text{F, Cl}$ improper hydrogen bonding was found with contraction of the C–H bond, in agreement with both models. The situation is, however, different for $X = \text{Br, I}$ where full calculations give evidence for the formation of the classical hydrogen bond (i.e., elongation of the C–H bond), while the electrostatic model provides contraction of the C–H bonds.

The NBO analysis tells us that the hydrogen bonding is a direct process where the primary effect is the EDT from the proton acceptor to the $X\text{--H}$ antibonding orbital of the proton donor. An increase in the electron density in this orbital leads to the weakening of the $X\text{--H}$ bond accompanied by its elongation. The improper hydrogen bonding represents, on the other hand, a more complicated “two-step” process. The charge transfer from the lone pairs of the electron donor is mainly directed to the lone electron pairs or antibonding orbitals in the remote (nonparticipating) part of the complex, which causes the elongation of bond(s) in that part of the complex. This primary effect is accompanied by the secondary effect of the structural reorganization of the proton donor, resulting in the contraction of the $X\text{--H}$ bond and the blue shift of the $X\text{--H}$ stretch frequency.

The different pattern of EDT in hydrogen-bonded and improper hydrogen-bonded complexes can be utilized to introduce an index which discriminates between both types of hydrogen bonding. The so-called hydrogen index [37] is defined as the ratio of electron density transferred from the proton acceptor to the σ^* antibonding orbital of the $X\text{--H}$ bond and the total electron density transferred between proton acceptor and proton donor. The value of the hydrogen index for standard hydrogen bonding lies between 1.0 and 0.7, while values below 0.3 are typical for improper blue-shifting hydrogen bonding. The criteria just given were derived using the NBO analysis performed at the MP2/6–31G* level (the NBO analysis was performed for the optimized complex and the optimized isolated proton donor). It is evident that the hydrogen index depends on the computational level and can be compared strictly only within one computational scheme. Values of the hydrogen index and shifts of the $X\text{--H}$ stretch frequency for a broad set of hydrogen-bonded and improper hydrogen-bonded complexes are presented in Table 2. In order to include also heavy atoms, the analysis was performed at the MP2/SDD** level. The table shows that the criteria are reasonable. All standard hydrogen-bonded complexes have a hydrogen index close to 1 and for the improper hydrogen-bonded complexes the hydrogen index drops to 0 or is even slightly negative. Water... HCBBr_3 and water... HClI_3 complexes belong, using the C–H stretch

Table 2. Hydrogen index, the change in the $X\text{--H}$ stretch frequency and total electron-density transfer (EDT) between proton acceptor and proton donor for various standard and improper hydrogen-bonded complexes. All the calculations were performed at the MP2/SDD** level. The hydrogen index is the ratio of the electron density transferred from the proton acceptor to the $X\text{--H}$ antibonding orbital of the proton donor and the total EDT

| Complex | Hydrogen index | $\Delta\nu(X\text{--H})$ (cm^{-1}) ^a | EDT (e) |
|--|----------------|---|----------------|
| $\text{H}_2\text{O}\dots\text{HCF}_3$ | 0.029 | 29 | 0.0090 |
| HCCl_3 | −0.039 | 26 | 0.0090 |
| HCBBr_3 | 0.194 | −20 | 0.0163 |
| HClI_3 | 0.302 | −36 | 0.0163 |
| HOH^b | 0.880 | −78 | 0.0207 |
| | | −37 | |
| HF | 0.966 | −299 | 0.0313 |
| HCl | 0.962 | −153 | 0.0261 |
| HBr | 0.970 | −168 | 0.0268 |
| HI | 1.038 | −115 | 0.0208 |
| $\text{Benzene}\dots\text{HCF}_3$ | −0.164 | 68 | 0.0049 |
| HCCl_3 | 0.002 | 57 | 0.0017 |
| HOH^b | 1.389 | −14 | 0.0023 |
| | | −23 | |
| $\text{Cl}^-\dots\text{H}_3\text{CBr}$ | −0.030 | 72 | 0.0730 |
| HCH_3 | 0.644 | −70 | 0.0284 |

^a Positive numbers indicate a blueshift

^b For H_2O as a proton donor both symmetric and antisymmetric stretches can be identified in the monomer and in the dimer. In the first line the change in the symmetric stretch is shown; the next line gives the change in the antisymmetric stretch frequency

frequency shift, among the hydrogen-bonded complexes, but the hydrogen index lies within the region of improper hydrogen-bonded complexes. Does this mean that criteria mentioned earlier are not valid? The answer is no. From the NBO analysis it is evident that for these two complexes (as well as for the other water... HCX_3 and many other complexes) two competing processes exist. First, EDT to the $X\text{--H}$ σ^* antibonding orbital (characteristic for hydrogen bonding) leads to the elongation of the $X\text{--H}$ bond and the red shift of the $X\text{--H}$ stretch frequency. Second, additional EDT to the remote part of the proton donor (characteristic for the improper hydrogen bonding) leads, via structural reorganization of the proton donor, to the contraction of the $X\text{--H}$ bond and the blue shift of the $X\text{--H}$ stretch frequency. The final value of the $X\text{--H}$ stretch frequency thus depends on the balance of the two processes. Evidently, for fluoroform and chloroform it is the latter process which dominates, while for bromoform and iodoform it is the former process.

4 Analysis of MOs

The NBO model is known to overestimate the role of charge transfer. The most straightforward method not affected by theoretical construction represents the analysis of MOs; however, the orbital analysis is possible only for the self-consistent-field (SCF) type of wave functions. If the SCF description is not valid (dispersion energy forms a large portion of the total interaction energy), the orbitals and the corresponding orbital energies could not be drawn.

We can consider the complex MOs as a linear combination of the subsystem (fragment) orbitals. The interaction (mixing) of the occupied orbitals of one subsystem with the virtual orbitals of the other subsystem leads to the intersystem EDT with the structural consequences discussed previously.

The orbital interaction picture for the standard hydrogen-bonded complexes, well known from textbooks on physical chemistry [38], is, owing to the use of orbital energies for localized MOs, not fully adequate. The interaction scheme is illustrated for the water...water complex. In the textbook picture, the lone pair (or generally an electron-rich orbital) of the proton acceptor mixes mainly with two orbitals of the proton donor: with the $X-H$ σ bonding orbital and to some extent with the $X-H$ σ^* antibonding orbital. All these orbitals are close to the HOMO-LUMO gap and the orbital energy difference is favorable for a relatively strong mixing. The three-orbital pattern with two occupied (lone-pair and σ) orbitals and one vacant (σ^*) orbital results in three new complex orbitals, if a localized picture is used. The lowest one is mainly the original σ orbital combined in phase with the lone-pair orbital. The energy of this new orbital is lower than the original σ orbital and the decrease in orbital energy represents the main stabilization of the complex. The next, again doubly occupied complex orbital strongly mixes all three fragment orbitals. The inclusion of the vacant σ^* orbital into the occupied space leads to the EDT from the lone pair to the region of the $X-H$ bond and also to the internal polarization in the proton-donor molecule, making the H atom more acidic in the complex than in the monomer. The picture is more complex, if delocalized, canonical orbitals are used (Fig. 2). The two highest occupied orbitals of the proton-acceptor water molecule interact mainly with the highest a_1 orbital of the proton donor. The combination of the two lowest vacant orbitals of the proton donor (which forms a localized O-H σ^* orbital) is mixed into the new HOMO-1 orbital of the complex. The resulting orbitals are identical with the simplified localized picture. The EDT, which is the consequence of the occupied-vacant orbital mixing, is clear.

The situation is similar in the case of the improper complexes; however, the participation of the vacant orbitals in the orbital mixing is smaller owing to the fact that the distances between the monomers are larger than in the case of the classical hydrogen-bonded complexes. The overlap between fragment orbitals in the improper complexes is thus about 1 order of magnitude smaller than in the classical complexes. Also the relative orbital energies are usually not very favorable.

The orbital interaction scheme is illustrated for the water...HCF₃ complex (Fig. 3). The C-H antibonding orbital is about 2 eV higher in the case of the water...HCF₃ complex than in the water dimer complex. The orbital mixing leads to an unusual EDT to the remote part of the proton-donor molecule (as a consequence of the delocalization of the C-H bonding orbital) and to the internal polarization of both interacting partners. Note that the EDT in the improper complexes is not a typical through-space process; rather, it is the result of the direct overlap between fragment orbitals, which are partly delocalized to the remote part of the proton donor, and

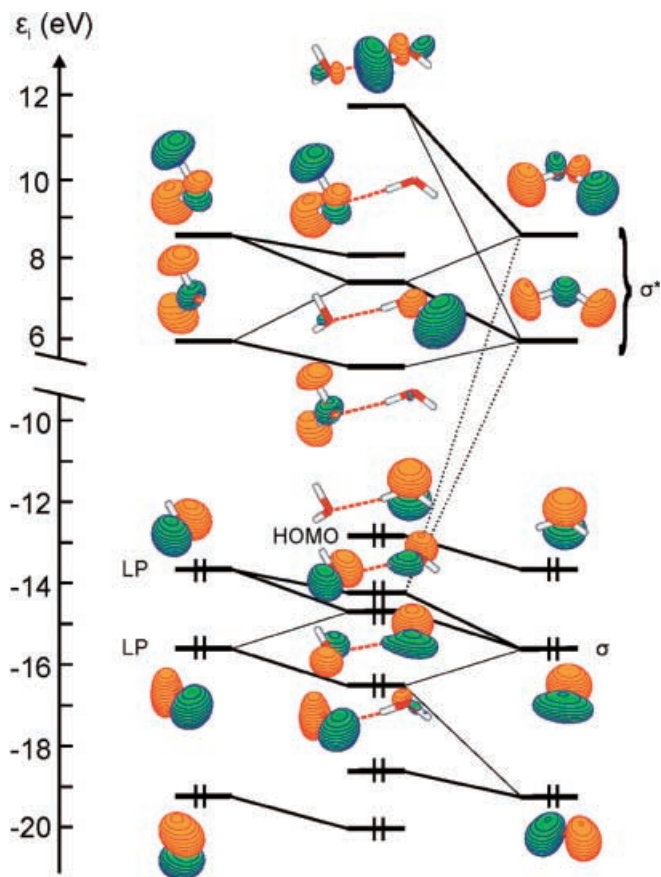


Fig. 2. Orbital interaction diagram of the water dimer. The orbitals and orbital energies were evaluated at the SCF/SDD** level

internal polarization resulting from the mixing of the orbitals of the same fragment. The situation is clear only for the strong complexes, like the anion-molecule complexes. In the case of the $Cl^- \dots H_3CBr$ improper hydrogen bond there is strong fragment orbital mixing between the HOMO orbital of the Cl^- (one of the degenerate p orbitals directed towards methylbromide along its C_3 axis) and the LUMO orbital of methylbromide (C-Br antibonding σ^* virtual orbital). These interacting fragment orbitals form the HOMO of the complex, in which the electron density on Cl^- decreases and the density on CH_3Br increases. The EDT into the C-Br antibonding orbital results in elongation of the C-Br bond, which, as discussed earlier, has consequences in the structural reorganization of the subsystem and finally in the blue shift of the C-H stretch vibrations.

5 Perturbational treatment of standard hydrogen bonding and improper, blue-shifting hydrogen bonding

In order to find differences between hydrogen-bonded and improper, blue-shifted hydrogen-bonded complexes (specifically, to find whether the contribution of various energy terms is comparable in both complexes) we performed the symmetry-adapted perturbation theory (SAPT) [38] analysis for the water dimer and the

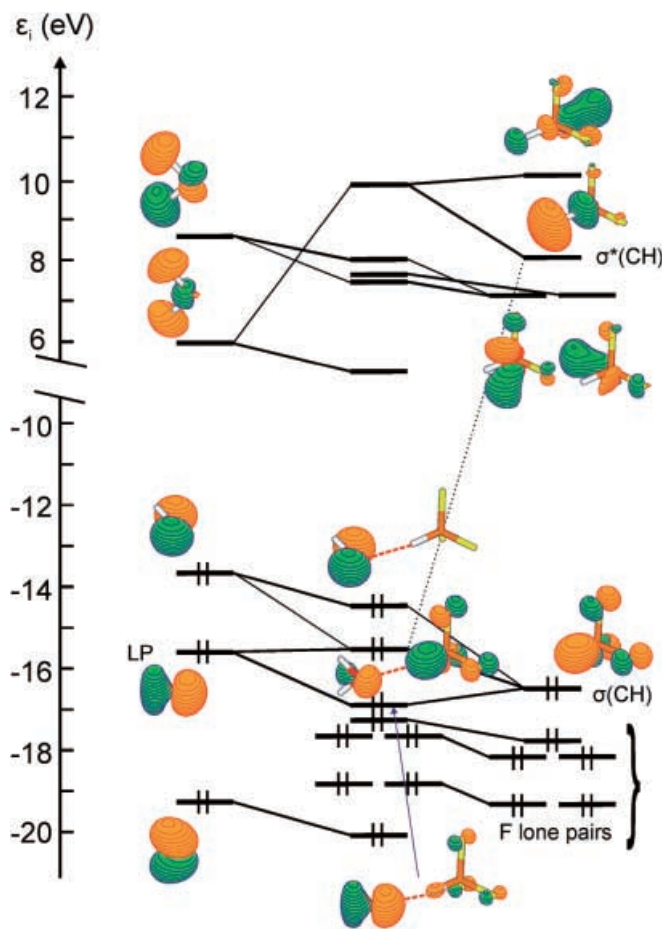


Fig. 3. Orbital interaction diagram of the water...HCF₃ complex. The orbitals and orbital energies were evaluated at the SCF/SDD** level

water...HCF₃ complex. From Table 3 we can find some differences between these two complexes which are, however, not too significant. The most important one concerns the induction energy, which is more important for the water dimer, where it forms more than 60% of the interaction energy. In the case of the HCF₃...water complex it is less than 30%. This difference indicates that the charge transfer in the former complex is more important than in the latter one, which fully agrees with the previously mentioned conclusion. Also the relative importance of the dispersion energy is different, being larger in the case of the water dimer. Obviously, the SAPT analysis confirmed the general conclusions of the theory of intermolecular interactions. The standard and the improper, blue-shifting hydrogen-bonded complexes do not differ considerably, and both types of complexes do not differ from the other intermolecular complexes.

6 Experimental verification of the two-step mechanism of improper, blue-shifting hydrogen bonding

The first experimental verification of the predicted blue shift was done for HCF₃...benzene and HCF₃...fluorobenzene complexes. Experiments in the gas phase did not allow the full verification of the previously

Table 3. Components of the interaction energy in the water dimer (standard hydrogen-bonded complex) and HCF₃...water (improper hydrogen-bonded complex) from the symmetry-adapted perturbation theory calculations (kcal/mol)

| | H ₂ O...HOH | H ₂ O...HCF ₃ |
|----------------------|------------------------|-------------------------------------|
| Electrostatic | -7.31 | -4.53 |
| Induction | -2.72 | -1.11 |
| Dispersion | -2.28 | -1.51 |
| Total attraction | -12.31 | -7.15 |
| Exchange-repulsion | 7.83 | 3.43 |
| First-order exchange | 6.84 | 3.13 |
| Exchange-induction | 1.39 | 0.48 |
| Exchange-deformation | -0.73 | -0.33 |
| Exchange-dispersion | 0.33 | 0.16 |
| Total | -4.47 | -3.71 |

mentioned two-step mechanism of the improper blue-shifted hydrogen bonding because they only provided information on the blue shift of the X-H stretch frequency upon complexation. The reason was that highly accurate gas-phase IR experiments have a rather narrow window for IR measurements, usually between 3,000 and 4,000 cm⁻¹, while for the verification of the previously mentioned mechanism a much broader window is required to detect also the C-X stretches. The respective verification was thus performed for the dimethyl ether (DME)...HCF₃ complex measured in liquid argon (cryogenic IR spectroscopy) [26]. The optimized structure of the complex is given in Fig. 4 and Fig. 5 presents the measured IR spectra. The formation of the complex leads to an increase in the C-H stretch frequency. Besides this blue shift a red shift of the C-O stretch and the C-O-C bend in DME and the C-F stretch in fluoroform is also apparent. How can we explain these frequency shifts in fluoroform and DME? By performing the NBO analysis we found a dominant EDT from the DME oxygen lone electron pairs to the lone electron pairs of the fluorine atoms of fluoroform. This shift results in weakening of all the C-F bonds, which is accompanied by their elongation and concomitant red shifts of their stretch vibrations. This primary effect leads to geometrical reorganization of the

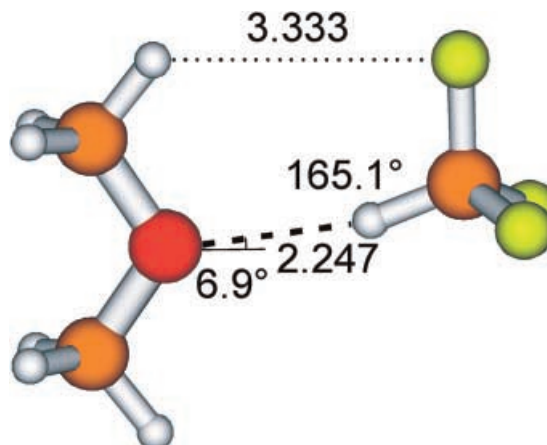


Fig. 4. Structure of the (CH₃)₂O...HCF₃ complex

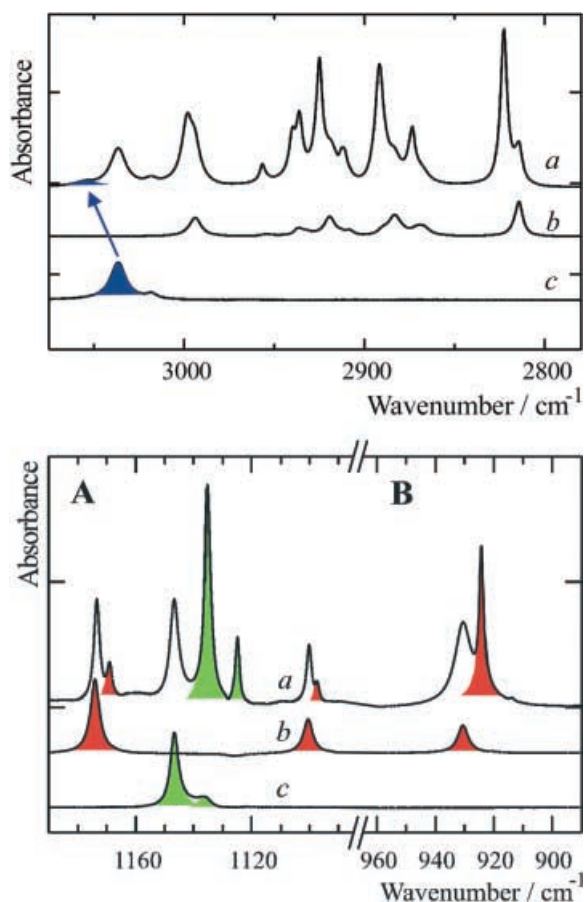


Fig. 5. IR spectrum of the the $(\text{CH}_3)_2\text{O}\cdots\text{HCF}_3$ complex [26]. The upper panel shows the C–H stretch region; the lower panel shows the C–F and C–O stretch regions (A) and the C–O–C bend region. (a) complex spectrum, b dimethyl ether spectrum, c HCF_3 spectrum)

fluoroform subsystem, where the contraction of the C–H bond represents the most evident feature. The contraction of the C–H bond is connected with the blue shift of this stretch frequency. The NBO analysis further revealed that the EDT from the DME oxygen should lead to weakening of both C–O bonds in DME; this is demonstrated by the red shifts of both stretch frequencies. Finally, weakening of the C–O bonds should be accompanied by a strengthening of all the C–H bonds in both DME methyl groups with concomitant blue shifts of these C–H stretch frequencies. Remarkable agreement between all experimental and theoretical vibration shifts justifies the proposed two-step mechanism of improper, blue-shifting hydrogen bonding.

7 Conclusion

Standard hydrogen bonding of the type $X\text{--H}\cdots Y$ is characterized by weakening of the $X\text{--H}$ bond, which causes elongation of this bond and a red shift of the $X\text{--H}$ stretch frequency. The improper, blue-shifting $X\text{--H}\cdots Y$ hydrogen bond is, on the other hand, characterized by the strengthening of the $X\text{--H}$ bond, which causes contraction of this bond and a blue shift of the $X\text{--H}$

stretch frequency. Both types of hydrogen bonds are characterized by EDT from the proton acceptor (Y) to the proton donor ($X\text{--H}$). This EDT is mostly larger for standard hydrogen-bonded systems (Table 2), where the dominant part of the EDT from lone electron pairs or regions of π electrons is directed to the $X\text{--H}$ σ^* antibonding orbital of the proton acceptor. The increase in the electron density in the σ^* orbital causes weakening of the $X\text{--H}$ bond and its elongation and the concomitant red shift of the $X\text{--H}$ stretch frequency. The situation is basically different in the case of improper, blue-shifting hydrogen bonding. The dominant part of the EDT is directed to a remote (nonparticipating) part of the proton-donor molecule, mostly to $R\text{--}X$ σ^* antibonding orbitals or to lone electron pairs of atom(s) in groups R , which are not directly involved in the $X\text{--H}\cdots Y$ contacts. There is negligible or only small EDT to the $X\text{--H}$ σ^* antibonding orbital. This primary effect is followed by a secondary effect: structural reorganization of the proton-donor framework with contraction of the $X\text{--H}$ bond directly involved in the $X\text{--H}\cdots Y$ contact and a concomitant blue shift of its stretch frequency. The formation of the standard hydrogen bond is thus a direct process and the weakening of the $X\text{--H}$ bond is a consequence of EDT. The formation of the improper, blue-shifting hydrogen bonding is, on the other hand, an indirect process where the strengthening of the $X\text{--H}$ bond results from structural reorganization induced by EDT from the donor to a remote part of the proton donor. Owing to the simple mechanism of the standard hydrogen bonding there are various correlations between the $X\text{--H}$ bond elongation and shift of the $X\text{--H}$ stretch frequency or stabilization energy. Such correlation does not exist in the case of improper hydrogen bonding owing to fact that only rarely is the electron density transferred solely to the remote part of the proton donor. The electron density is mostly distributed between a remote part and the $X\text{--H}$ σ^* antibonding orbital. The different target of EDT in hydrogen-bonded and improper hydrogen-bonded complexes is also reflected by different regions where the dominant geometry changes take place. In the case of standard complexes, it is the $X\text{--H}$ bond of the proton donor, while in the improper complexes it is the remote (nonparticipating) part of the proton donor.

The electrostatic model predicts basically the correct direction of the changes for both types of complexes, but the predicted changes are largely underestimated or overestimated and the model sometimes fails completely.

The similar features of the hydrogen-bonded and improper hydrogen-bonded complexes which justify the use of the term “hydrogen bond” in both cases are

1. The position of the hydrogen between two electro-negative atoms.
2. EDT from the proton acceptor to proton donor.
3. The stability of the complex.
4. The directionality of $X\text{--H}\cdots Y$ contacts.
5. The role of the electrostatic field.

On the other hand, the different features of the improper hydrogen-bonded complexes which support the use of the additional specification “improper, blue-shifting” are

1. The strengthening of the $X-H$ bond (instead of weakening).
2. The contraction of the $X-H$ bond (instead of elongation).
3. The blue shift of the $X-H$ stretch frequency (instead of a red shift).
4. EDT to the remote (not participating) part of the proton donor (instead of to the $X-H$ bond).
5. The dominant geometry change in the remote (not participating) part of the proton donor and the corresponding vibrational frequency shifts in the remote part.

Acknowledgements. This project, LN00A032 (Center for Complex Molecular Systems and Biomolecules), was supported by the Ministry of Education of the Czech Republic. We acknowledge Robert Moszczynski for performing the SAPT calculations for the water dimer and the water...HCF₃ complex.

References

1. Jeffrey GA (1997) An introduction to hydrogen bonding. Oxford University Press, New York
2. Desiraju GR, Steiner T (1999) The weak hydrogen bond. Oxford University Press, Oxford
3. Scheiner S (1997) Hydrogen bonding. Oxford University Press, New York
4. Pauling L (1931) J Am Chem Soc 53: 1367
5. Suzuki S, Green PG, Bumgarner RE, Dasgumpta S, Goddard WA III, Blake GA (1992) Science 257: 942
6. Pribble RN, Garret AW, Haber K, Zwier TS (1995) J Chem Phys 103: 531
7. Djafari S, Lembach G, Barth H-D, Brutschy B (1996) Z Phys Chem 195: 253
8. Djafari S, Barth H-D, Buchhold K, Brutschy B (1997) J Chem Phys 107: 10573
9. Legon AC, Wallwork AL, Warner HE (1992) Chem Phys Lett 191: 97
10. Legon AC, Roberts BP, Wallwork AL (1990) Chem Phys Lett 173: 107
11. Steiner T, Desiraju GR (1998) Chem Commun 891
12. (a) Steiner T, et al (1996) J Chem Soc Perkin Trans 2 2441; (b) (1992) J Chem Phys 96: 1787; (c) (1995) J Chem Soc Perkin Trans 2 1321; (d) (192) J Chem Phys 96: 7321; (e) (1997) J Am Chem Soc 119: 4232
13. Hobza P, Havlas Z (2000) Chem Rev 100: 4253
14. Trudeau GT, Dumas J-M, Dupuis P, Guerin M, Sandorfy C (1980) Top Curr Chem 93: 91
15. Budešinský M, Fiedler P, Arnold Z (1989) Synthesis 858
16. Boldeskul IE, Tsybal IF, Ryltsev EV, Latajka Z, Barnes AJ (1997) J Mol Struct (THEOCHEM) 167: 436
17. Hobza P, Špirko V, Selzle HL, Schlag EW (1998) J Phys Chem A 102: 2501
18. Hobza P, Špirko V, Havlas Z, Buchhold K, Reimann B, Barth H.-D, Brutschy B (1999) Chem Phys Lett 299: 180
19. Reimann B, Buchhold K, Vaupel S, Brutschy B, Havlas Z, Hobza P (2001) J Phys Chem A 105: 5560
20. Hobza P, Havlas Z (1999) Chem Phys Lett 303: 447
21. Gu Y, Scheiner S (1999) J Am Chem Soc 121: 9411
22. Karger A, Amorim da Costa AM, Ribeiro-Claro PJA (1999) J Phys Chem A 103: 8672
23. Mizuno K, Imafuji S, Ochi T, Ohta T, Maeda S (2000) J Phys Chem B 104: 11001
24. Masunov A, Dannenberg JJ, Contreras RH (2001) J Phys Chem A 105: 4737
25. Hartmann M, Wetmore SD, Radom L (2001) J Phys Chem A 105: 4470
26. Van der Veken BJ, Herrebout WA, Szostak R, Shchepkin DN, Havlas Z, Hobza P (2001) J Am Chem Soc 123: 12290
27. Zierkiewicz W, Michalska D, Havlas Z, Hobza P (2002) Chem Phys Chem 3: 511
28. Pohle W, Gauger DR, Fritzsche H, Rattay B, Selle C, Binder H, Böhlig H (2001) Mol Struct 563–564: 463
29. Ford TA, Glasser LJ (1997) J Mol Struct (THEOCHEM) 398–399: 381
30. Caminati W, Melandri S, Moreschini P, Favero PG (1999) Angew Chem Int Ed Engl 38: 2924
31. Alkorta I, Rozas I, Elguero J (2002) Int J Quantum Chem 86: 122
32. Coulson CA (1957) Res Appl Ind 10: 149
33. Reed AE, Curtiss LA, Weinhold F (1988) Chem Rev 88: 899
34. Bader RWF (1990) Atoms in molecules. A quantum theory. Oxford University Press, Oxford
35. Cubero E, Orozco M, Hobza P, Luque FJ (1999) J Phys Chem A 103: 6394
36. Cubero E, Orozco M, Luque FJ (1999) Chem Phys Lett 310: 445
37. Hobza P (2001) Phys Chem Chem Phys 3: 2555
38. Atkins PW (1998) Physical chemistry. Oxford University Press, New York
39. Jeziorski B, Moszczynski R, Szalewics R (1994) Chem Rev 94: 1887